2003-06

Barrel wear reduction in rail guns: the effects of known and controlled rail spacing on low voltage electrical contact and the hard chrome plating of copper-tungsten rail and pure copper rails

NAVAL POSTGRADUATE SCHOOL
Monterey, California

THESIS

BARREL WEAR REDUCTION IN RAIL GUNS: THE EFFECTS OF KNOWN AND CONTROLLED RAIL SPACING ON LOW VOLTAGE ELECTRICAL CONTACT AND THE HARD CHROME PLATING OF COPPER – TUNGSTEN RAIL AND PURE COPPER RAILS

by

Cedric J. McNeal

June 2003

Thesis Advisor: William B. Maier II
Co-Advisor: Richard Harkins

Approved for public release; distribution is unlimited.

THIS PAGE INTENTIONALLY LEFT BLANK

REPORT DOCUMENTATION PAGE

Form Approved OMB No. 0704-0188

1. AGENCY USE ONLY *(Leave blank)*	2. REPORT DATE	3. REPORT TYPE AND DATES COVERED
	June 2003	Master's Thesis

4. TITLE AND SUBTITLE Barrel Wear Reduction in Rail Guns: An Investigation of Sliding Electrical Contact and the Hard Chrome Plating of a Copper- Tungsten Rail

5. FUNDING NUMBERS

6. AUTHOR(S) McNeal, Cedric J

7. PERFORMING ORGANIZATION NAME(S) AND ADDRESS(ES)
Naval Postgraduate School
Monterey, CA 93943-5000

8. PERFORMING ORGANIZATION REPORT NUMBER

9. SPONSORING / MONITORING AGENCY NAME(S) AND ADDRESS(ES)
N/A

10. SPONSORING/MONITORING AGENCY REPORT NUMBER

11. SUPPLEMENTARY NOTES The views expressed in this thesis are those of the author and do not reflect the official policy or position of the U.S. Department of Defense or the U.S. Government.

12a. DISTRIBUTION / AVAILABILITY STATEMENT
Approved for public release; distribution is unlimited.

12b. DISTRIBUTION CODE

13. ABSTRACT ***(maximum 200 words)***

Barrel wear at the rail-projectile interface continues to hinder the development of a practical rail gun. Previous research at the Naval Postgraduate School tested barrel wear for current densities up to 28,500 kA/cm^2 with selected interface materials at low velocities (<100 m/s). Low voltage electrical contact was not maintained for some experimental shots and non-parallel rails were the suspected cause. In this thesis, we used a non-contact capacitive sensor to determine rail spacing to within $\pm 10 \mu m$, so that the rails will be parallel within small tolerances. Several rails were used in these experiments: 75-25 copper-tungsten, chromium-plated 75-25 Cu-W, and chromium-plated pure copper rails. Improving the control of rail spacing and parallelity did not ensure low-voltage electrical contact for our configurations. The largest damage was observed for chromium-plated copper rails and the least damage occurred for chromium-plated 75-25 Cu-W rails.

14. SUBJECT TERMS	15. NUMBER OF PAGES
Rail gun, low voltage electrical contact, non-contact capacitive sensor, hard chrome plating	65
	16. PRICE CODE

17. SECURITY CLASSIFICATION OF REPORT	18. SECURITY CLASSIFICATION OF THIS PAGE	19. SECURITY CLASSIFICATION OF ABSTRACT	20. LIMITATION OF ABSTRACT
Unclassified	Unclassified	Unclassified	UL

NSN 7540-01-280-5500 **Standard Form 298 (Rev. 2-89)**
Prescribed by ANSI Std. 239-18

THIS PAGE INTENTIONALLY LEFT BLANK

Approved for public release; distribution is unlimited

BARREL WEAR REDUCTION IN RAIL GUNS: THE EFFECTS OF KNOWN AND CONTROLLED RAIL SPACING ON LOW VOLTAGE ELECTRICAL CONTACT AND THE HARD CHROME PLATING OF COPPER – TUNGSTEN RAIL AND PURE COPPER RAILS

Cedric J. McNeal
Lieutenant, United States Navy
B.S., Southern University and A&M College, 1997

Submitted in partial fulfillment of the
requirements for the degree of

MASTER OF SCIENCE IN APPLIED PHYSICS

from the

NAVAL POSTGRADUATE SCHOOL
June 2003

Author: Cedric J. McNeal

Approved by: William B. Maier II
Thesis Advisor

Richard Harkins
Co-Advisor

William B. Maier II
Chairman, Department of Physics

THIS PAGE INTENTIONALLY LEFT BLANK

ABSTRACT

Barrel wear at the rail-projectile interface continues to hinder the development of a practical rail gun. Previous research at the Naval Postgraduate School tested barrel wear for current densities up to 28,500 kA/cm^2 with selected interface materials at low velocities (<100 m/s). Low voltage electrical contact was not maintained for some experimental shots, and non-parallel rails were the suspected cause. In this thesis, we used a non-contact capacitive sensor to determine rail spacing to within $\pm 10 \mu m$, so that the rails would be parallel within small tolerances. Several grooved rails were used in these experiments: 75-25 Cu-W (copper-tungsten), chromium-plated 75-25 Cu-W, and chromium-plated pure copper rails. Improving the control of rail spacing and parallelity did not ensure low-voltage electrical contact for our configurations. The largest damage was observed for chromium-plated copper rails and the least damage occurred for chromium-plated 75-25 Cu-W rails.

THIS PAGE INTENTIONALLY LEFT BLANK

TABLE OF CONTENTS

THIS PAGE INTENTIONALLY LEFT BLANK

LIST OF FIGURES

LIST OF TABLES

THIS PAGE INTENTIONALLY LEFT BLANK

ACKNOWLEDGEMENTS

I would first and foremost like to thank God for being my provider and giving me the strength, mind, and knowledge to complete the research for this thesis.

Don Snyder is the person who has guided me and been the backbone for rail gun research here at the Naval Postgraduate School; and to him owe a great deal of gratitude for his relentless efforts, dedication to job accomplishment and technical insight. Other people I would like to thank nternal to NPS are George Jaksha for his professional attitude and extreme timeliness in the machining of materials, Nancy Weigle, Nancy Carroll, and Jiraphon Girrard for their expedient execution in ordering of materials, Richard Harkins for his assistance as second reader and most of all William Maier for his time and patience in allowing me to even conduct this research. External support from commercial manufacturers also played an integral role in the completion of this research and I would like to thank Dianne Positeri at Polcraft Inc. in San Jose, California, Jeff Peduzzi at Capacitec in Ayer, Massachusetts and Greg Barken at Barken’s Hard Chrome in Compton, California.

Lastly, I would like to thank my wife for her support. Her presence and understanding was truly instrumental to the completion of my furthering education here at NPS.

THIS PAGE INTENTIONALLY LEFT BLANK

I. INTRODUCTION

A. PURPOSE

This thesis further examines the interface between armature and barrel for Electromagnetic (EM) Rail Guns. A soft conductive material at the sliding electrical contact is used to reduce rail damage. Damage was examined for several shots by using the NPS 4-inch rail gun test stand, a commercial conductive paste, a silver-tungsten projectile, and three different types of rails. A manufactured non-contact capacitive sensor was used to help determine what gap distance between the rail and projectile brings about low-voltage electrical contact for each shot. The next step was to find at what current density breakdown would occur and examine damage for each type of rail while operating at velocities ranging from 35 – 70 m/s and currents ranging from 13 – 21 kiloamperes. And finally, the last step examines whether a hard chrome plated rail would improve performance. Achieving the goals of sliding electrical contact for each shot and finding the type of rail that will minimize damage will further enable research contributing to the Navy's desires of implementing an EM rail gun which has a barrel life of sustaining 2000 shots prior to barrel change out [1].

B. HISTORY

The beginnings of the concept of the Electromagnetic (EM) Gun date as far back as 1901 and also to that of an electromagnetic canon, which was built and tested in World War II [2]. Throughout the twentieth century, a number of

scientists and inventors have attempted to patent a “rail gun” but none have been able to patent a weapon to be integrated into the military.

Past research and attempts have brought us to today where electromagnetic guns, at some facilities in the United States and abroad, can fire projectiles at velocities exceeding 1.5 km/sec. However, many issues are still to be resolved, such as projectile size, makeup, and design, a power supply design and compatibility, cooling for the weapon, and most importantly, barrel wear at the interface between the projectile and rails.

C. NAVAL APPLICATIONS AND ADVANTAGES

As of mid-November 2002, the Chief of Naval Operations established an Electric Weapons Office, which has incorporated within it a division, which, is to manage the full-scale concept of the electro-magnetic rail gun [1]. An electromagnetic gun would clearly serve as weapon of choice for the United States Navy due to its numerous advantages over the current weapons systems in our fleet inventory. One advantage would be the elimination of the processes of ignition and combustion, which greatly hinder control features and limit gun performance.

Another advantage is that Electromagnetic guns will achieve extremely high velocities (ranging from 1.5 – 2.5 km/sec). The Navy’s new all electric ship concept would serve as a prime candidate for integrating this technology onboard a naval vessel. The nominal naval electromagnetic gun, when integrated onboard the electric ship, provides 17 MJ of energy on target, shoots 6 – 12 rounds per minute,

and has a range of 250 nautical miles for a flight time of approximately 6 minutes. As compared to current shipboard technology, which includes that of the Extended Range Guided Missile (ERGM), the electromagnetic gun would surpass its range by over 5 times at a cost per round, at substantially less cost per round than that of a long range missile or ERGM. The increased gun range and decreased response time will provide our naval fleet with increased littoral coverage for our Marines and increased stand – off capability for our Sailors [1].

D. RAILGUN THEORY

The basic understanding of EM gun theory can be simply explained from the fundamental observations made by Biot, Savart, and other scientists. The law of Biot and Savart, shown below in equation 1.1, gives the magnetic field, $\vec{B}$ caused by the current in the loop where the integration is along the current path in the direction of current flow, $d\vec{l}$ is an element of length along the wire (simplified), and $\hat{r}$ is a vector from $d\vec{l}$ to the point at the we evaluate the field, μ_0 is the permeability of free space $\left(4\pi \times 10^{-7} Tm/A\right)$ and I is the respective current. Actual magnetic field distributions can be estimated more accurately with QuickField Software designed by Tera Analysys Ltd.

$$\vec{B} = \frac{\mu_0}{4\pi} \int \frac{I(d\vec{l} \times \hat{r})}{r^2} \qquad (1.1)$$

Equation 1.2 gives the force on a current carrying wire in a magnetic field of strength *B*, and can be used to obtain the Lorentz Force on the projectile.

$$d\vec{F} = I(d\vec{l}' \times \vec{B}) \qquad (1.2)$$

where $d\vec{l}'$ is an element of length along the projectile. Figure 1 depicts the situation. This most basic configuration of a rail gun is two parallel conducting rails with a conducting, mobile projectile and the introduction of a current at the end of the rails. From this current, a magnetic field is generated. The projectile serves as a conducting path and carries current from the first rail to the second. The current in the projectile interacts with the magnetic field produced by the currents in the rails to give the Lorentz Force mentioned above. This force is usually written as:

$$F = \frac{1}{2} L' I^2 \qquad (1.3)$$

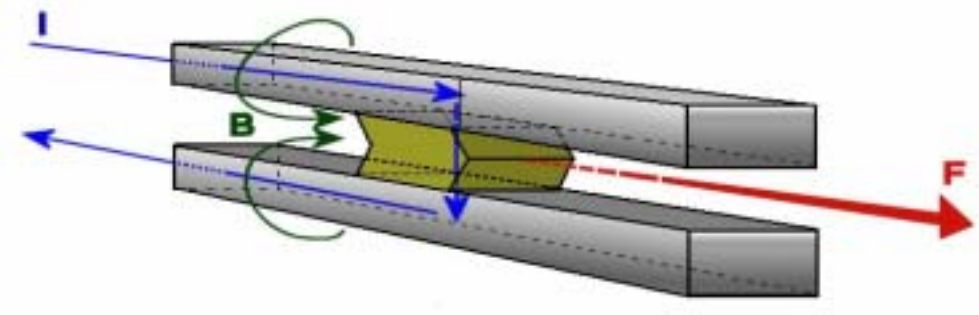

Figure 1. Lorentz Force Depiction.

where L' is the inductance gradient of the rail gun and is the of the order of 0.5 μH/m.

E. BARREL WEAR

The ongoing challenge of barrel wear at the rail-projectile interface continues to hinder the development of a practical rail gun. There are two major sources that contribute to problem of barrel wear.

The first is that of gouging during the launching of the projectile. Gouging is damage to the rail that occurs when surfaces (rail and projectile) come in contact with each other at high velocities or hypervelocity. This gouging has been a major problem in rail gun technology. Researchers Stefani and Parker, at the Institute for Advanced Technology (located in Austin, TX at the University of Texas) have discovered that the gouging is dependent upon the hardness of the harder material and by the density and speed of sound of both materials [3].

Additional barrel wear may come from the sliding of electrical contacts even at low velocities. Here, it has been observed that if the nature of the sliding electrical contact transitions from low voltage and liquid film interface to high voltage and plasma arc, then significant barrel damage will occur after the transition [4,5]. Maintenance of a low-voltage sliding liquid film interface is critical in determining the ideal projectile/armature design that will be most compatible with the selected rail/barrel design.

This thesis will further examine the use of a semi-liquid interface material to maintain low-voltage sliding electrical contact at low velocities (35 – 70 m/sec).

F. PROJECT OBJECTIVE

The overall objective of this thesis is to use the NPS rail gun test stand to identify a material whose use at the rail-projectile interface will maintain good electrical contact and minimize barrel erosion. The first step is to control those parameters, such as rail spacing, that influence electrical contact at the projectile-rail interface. The next step is discover the ideal interface material between the rail and projectile so that low-voltage electrical contact is maintained throughout the length of the rail and damage to the rail is small at current densities $\geq$ 25 kA/cm^2 (appropriate to a naval rail gun).

By accomplishing these goals, NPS would have developed a method that could be used to test interfaces quickly and possibly answer one of the Navy's EM rail gun issues.

II. EXPERIMENTAL APPROACH

A. EQUIPMENT

The experimental approach is to fire a small silver-tungsten projectile (current-carrying face with an area of 0.604 cm^2) along a rail (100-cm length) coated with a semi-liquid conducting medium (Conducto-Lube). All rails in this thesis were grooved, and diagrams of the two types of groove patterns can be seen in the Appendix. During a shot, we monitor the current through the projectile, the voltage drop across the rails, the time at which the projectile is fired and the time at which the projectile exits the rails. The equipment and procedures are detailed below.

The equipment used for this thesis has evolved over a period of about three years starting with the work of Don Gillich in June 2000 [6]. Improvements by Mark Adamy, include a ceramic spacer, which dramatically improved rail alignment and the addition of an accelerator/pusher assembly, (shown in figures 2 and 3), which allows the projectile to begin its movement prior to current being sent through the rails.

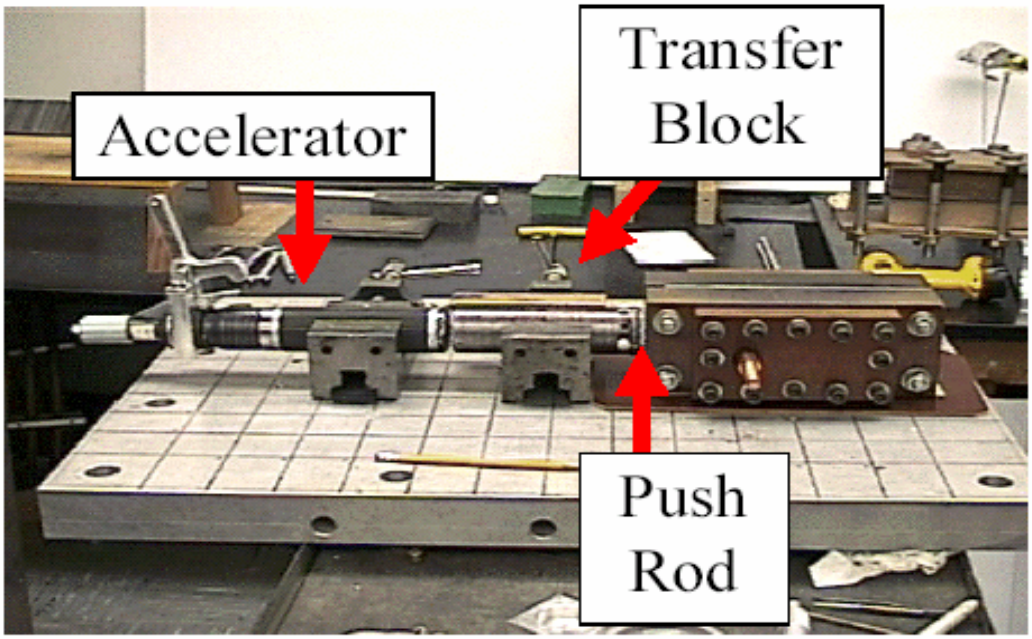

Figure 2. Accelerator Assembly Connected to NPS Rail Gun Test Stand.

The transfer block, another of Adamy's contributions, serves as a housing for the pusher assembly shown below [7].

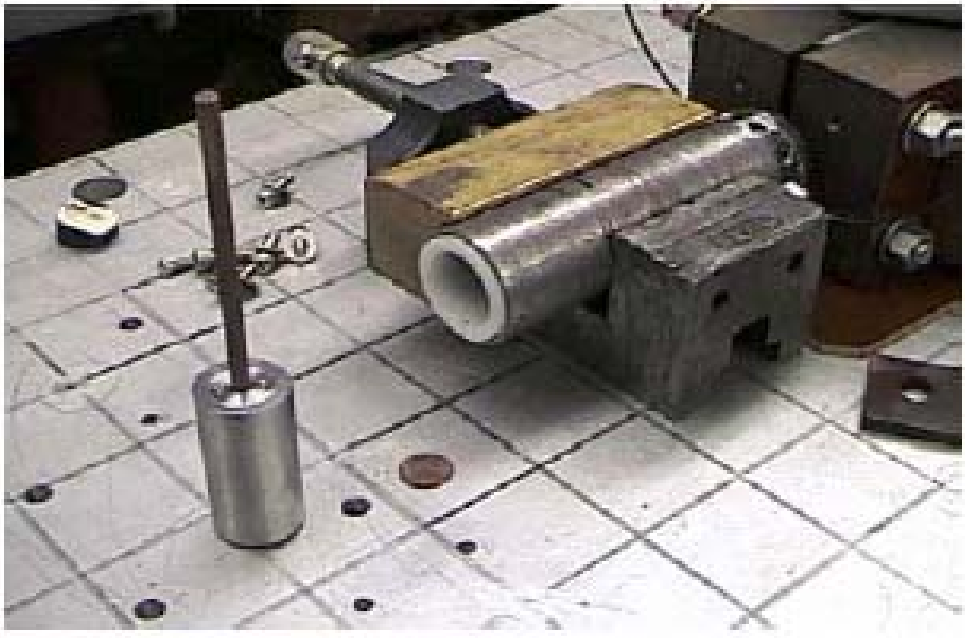

Figure 3. Pusher Assembly Placed Upright.

William Culpeper and Michael Smith contributed the use of the commercial silver paste, which reduced the amount of rail erosion and provided improved electrical contact and conductivity at the rail/projectile interface [4,5]. Low voltage electrical contact for different experimental shots was still not consistently achieved for the NPS rail gun test stand.

This thesis adds an upgrade to NPS rail gun test stand. A commercially manufactured non-contact capacitive sensor has been used to give known and controlled rail spacing to within $\pm 10 \mu m$. This upgraded test stand is used to test damage to both a 75-25 copper-tungsten alloy rail and to hard-chrome plated rails, which are significantly harder than Cu-W rails. With these elements, we explore rail degradation at current densities between 20 – 35 kA/cm^2.

1. Power Supply and Current Density

The major components of the power supply used to conduct research supporting this thesis are the same as described in the previous research conducted by Michael Smith [5]. Its schematic design is shown below and is described as follows.

Two parallel, 830 μF capacitors, rated at 11 kV provide a total capacitance of 1660 μF. The three diode strings of DA24 F2003 high power avalanche diodes prevent current reversal to the capacitors during discharge. A TVS-40 fast-acting vacuum switch connects the capacitors to

the rails through a total inductance of 32.5 μH (30 μH external inductor combined with the power supply's inherent inductance already existing 2.5 μH). A 0.03Ω resistive voltage divider placed across the rails provides a method of measuring voltages across the rails by using a differential amplifier and oscilloscope.

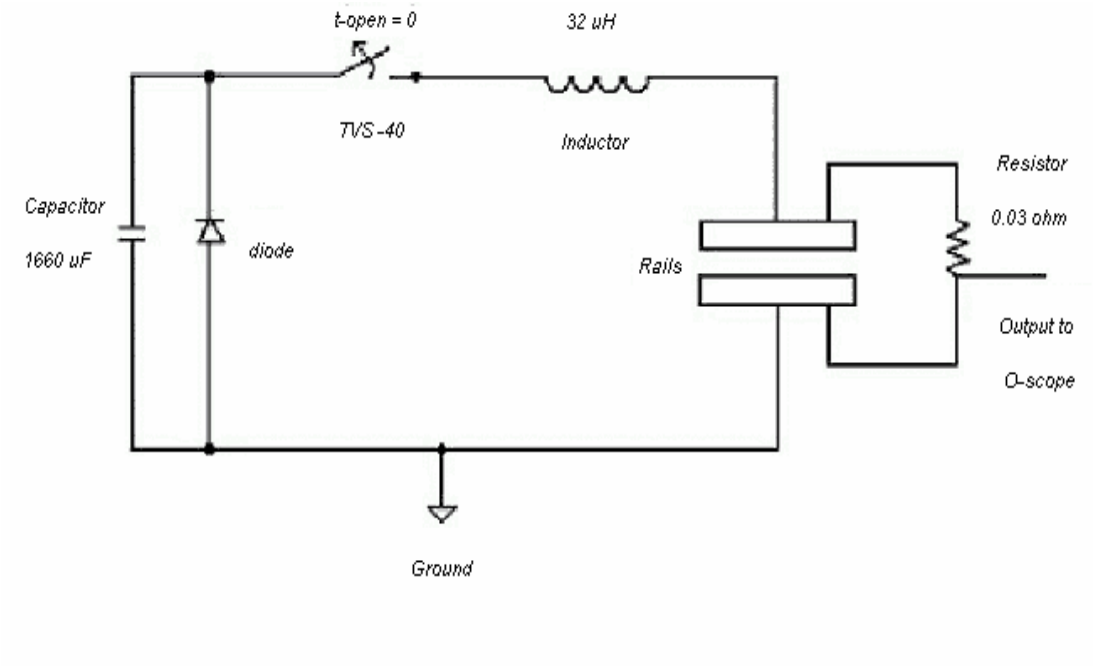

Figure 4. Schematic Diagram of the NPS Rail Gun Test Stand.

A Pearson Transformer provides a quantitative measurement of the current for each experimental shot. The Pearson Transformer's sensitivity factor is $5\frac{mV}{A}$, and we calculate current densities for each shot from:

$$I_{peak} = \frac{10V_{p-p}}{\frac{5mV}{Amp}} = \frac{2000V_{p-p}}{\frac{V}{Amp}} = 2000V_{p-p} \quad \text{[Amps]} \qquad (2.1)$$

where I_{peak} is the peak value of the current, V_{p-p} is peak to peak value of the voltage obtained from the oscilloscope reading, and the factor of 10 accounts for a 10:1 voltage divider which connects between the oscilloscope and Pearson Transformer to keep voltage readouts below 10 V [5]. Once peak current is obtained, it is divided by the projectile area (projectiles used have a current-carrying face with area 0.604 cm^2), which gives current density *J* and is shown below:

$$J = \frac{I_{peak}}{Area} \quad \left[\frac{Amps}{cm^2}\right] \tag{2.2}$$

2. Other NPS Rail Gun Components

As mentioned previously, numerous upgrades and contributions by past thesis students and Don Snyder to the current NPS EM rail gun assembly enable it to be used in the manner and capacity it is used today. In December 2001, Mark Adamy contributed the idea of using of a ME Schermer Captive Bolt Stunner, shown below in Figure 5.

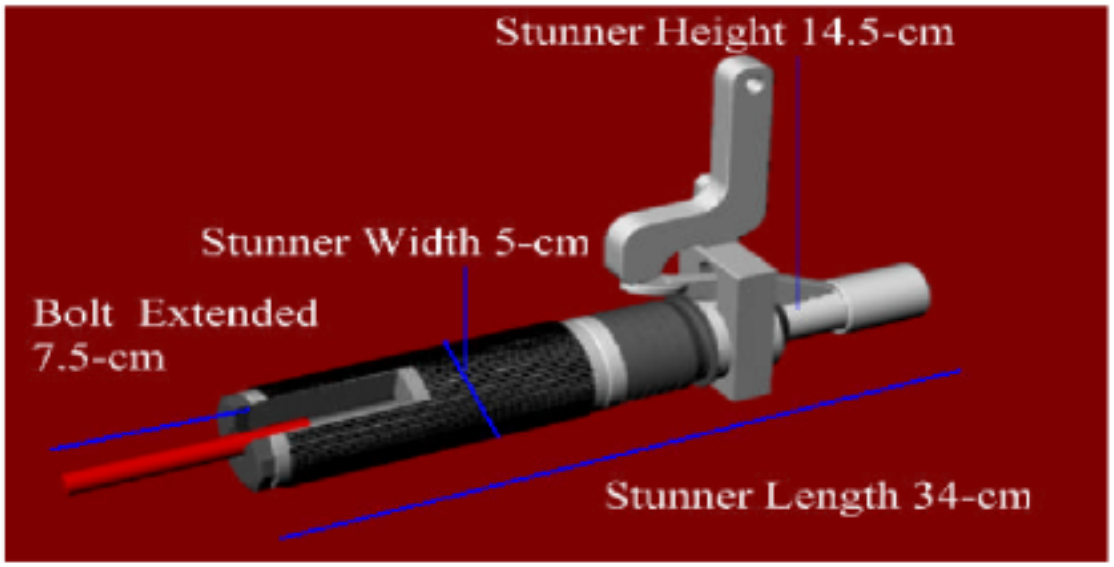

Figure 5. Depiction of the ME Schermer Captive Bolt Stunner.

This device acts as an accelerator and is able produce projectile velocity of up to about 70 m/s by use of a cartridge charge. The pusher housing and assembly together also act as a trigger so that when the pusher crosses a light beam, the TVS-40 switch is closed, by use of a trigger box and delay generator.

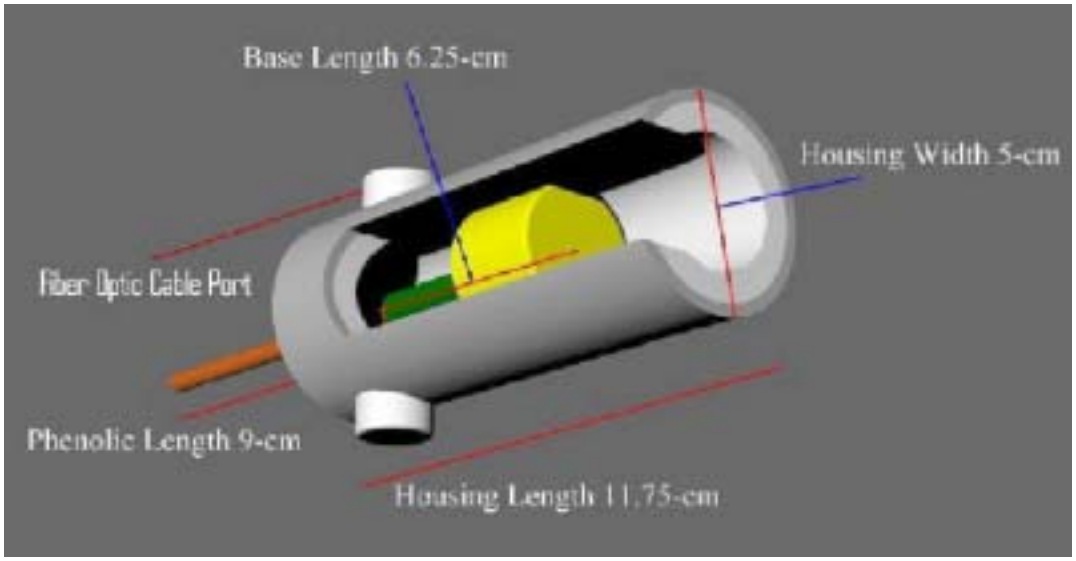

Figure 6. Depiction of the Pusher Housing.

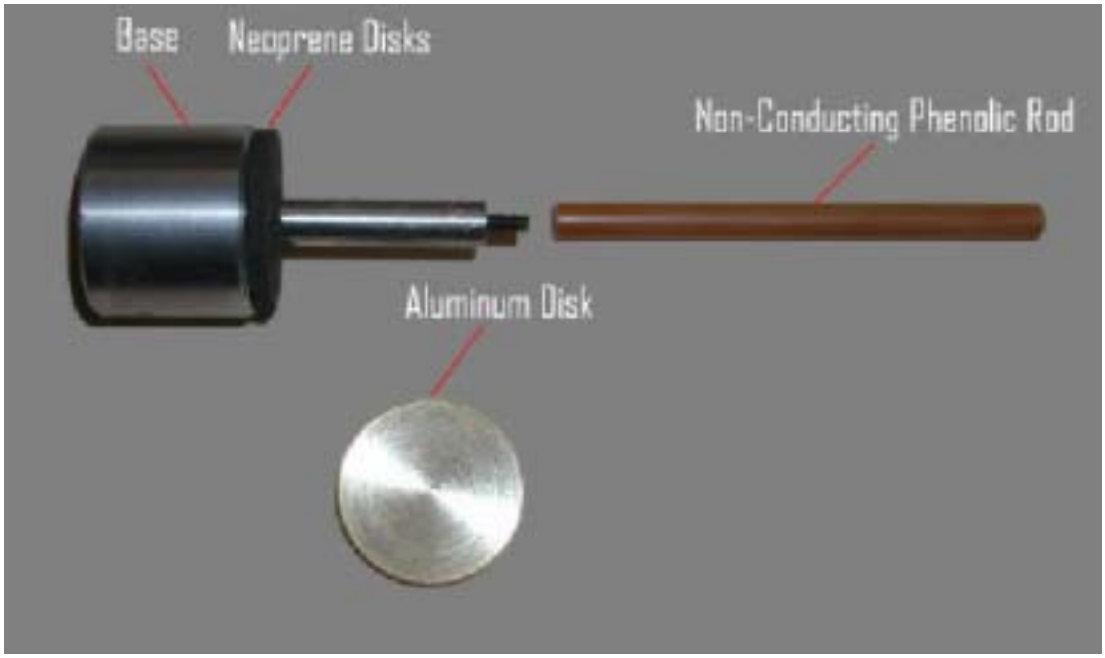

Figure 7. Depiction of the Pusher Assembly [7].

As previously stated, Culpeper contributed a method which allowed for the voltage across the rails to be measured by using a Lecroy DA1822A Differential Amplifier being placed in parallel with a 0.03Ω resistor and the rails. To completely allow for accurate measurements of the voltage drop across the rails, the differential amplifier is placed in parallel with a variable compressible graphite resistor, which as the 10:1 voltage divider accounted for in the previous calculation of I_{peak}. The graphite resistor is shown below in Figure 8.

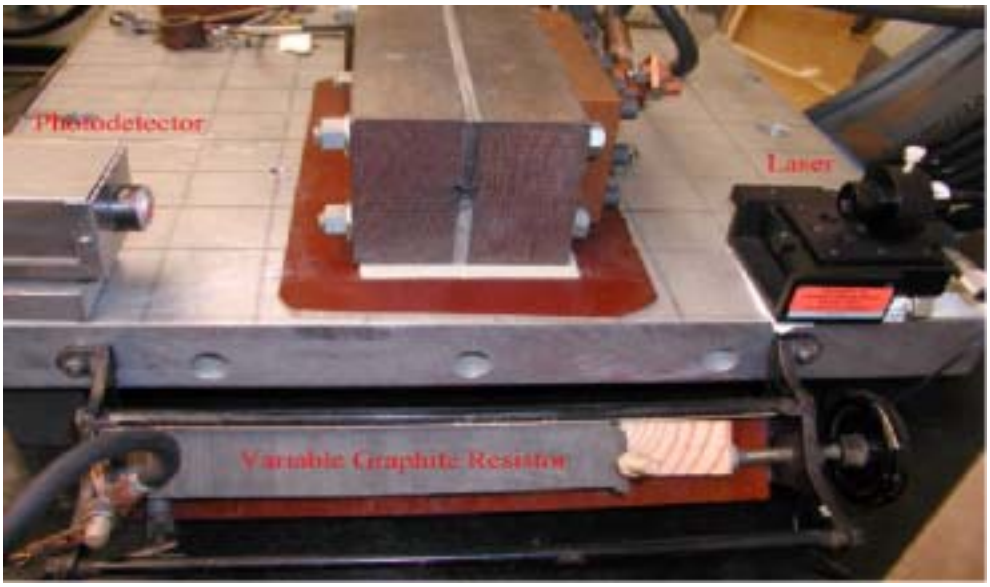

Figure 8. Depiction of the Muzzle End of the NPS Rail Gun Test Stand – Laser, Photodetector, and Variable Graphite Resistor.

Also shown in Figure 8 is the photo-detector and laser. These two components, along with the initial beam crossing of the pusher and then the projectile crossing of the laser beam depicted above allow for a time measurement, where the from the length traveled by the projectile is known, and allow for a velocity calculation [4].

B. UPGRADES AND IMPROVEMENTS TO THE NPS RAIL GUN

This research and experiments conducted in this thesis were based on the results and recommendations from previous research, more specifically Michael Smith's thesis. His conclusions suggested that a device for measuring the gap distance between the rails was needed to ensure a parallel path for the projectile while inside the rails. Smith's conclusions also noted that the copper-tungsten alloy used in his experiments, seemed to withstand currents up to

almost 19kA, which corresponds to a current density of $30\,kA/cm^2$ [5]. One of the goals of this thesis was to select another metal alloy for the make-up of the rail, one that would be harder, as measured by the Rockwell scale, and have a similar value of conductivity.

1. Non-Contact Capacitive Sensor

The focus of the research conducted in this thesis was geared first towards establishing a method by which low-voltage electrical contact could be obtained for experimental shots. A non-contact capacitive sensor was chosen to resolve the issue of rail parallelity and spacing. This sensor was advertised and manufactured by Capacitec. This device measures spacing between the rails at any given point along the 100-cm rails. This precise knowledge is needed for controlled study of low-voltage electrical contact.

The sensor provided by Capacitec consists of three major components: the non-contact capacitive sensing probe, its amplifier integrated into the power supply, and a Bargrafx software application which provides a graphical readout enabling the user to easily interpret gap distances between the rail and projectile and total separation distance between the two rails. To fit the NPS rail gun design, Capacitec mocked the 0.604 cm^2, silver-tungsten, projectile and embedded a capacitive sensor on either side. The non-contact capacitive sensing probe, attached to a plastic extension, which allows movement of the sensor throughout the path of the rails, is shown below.

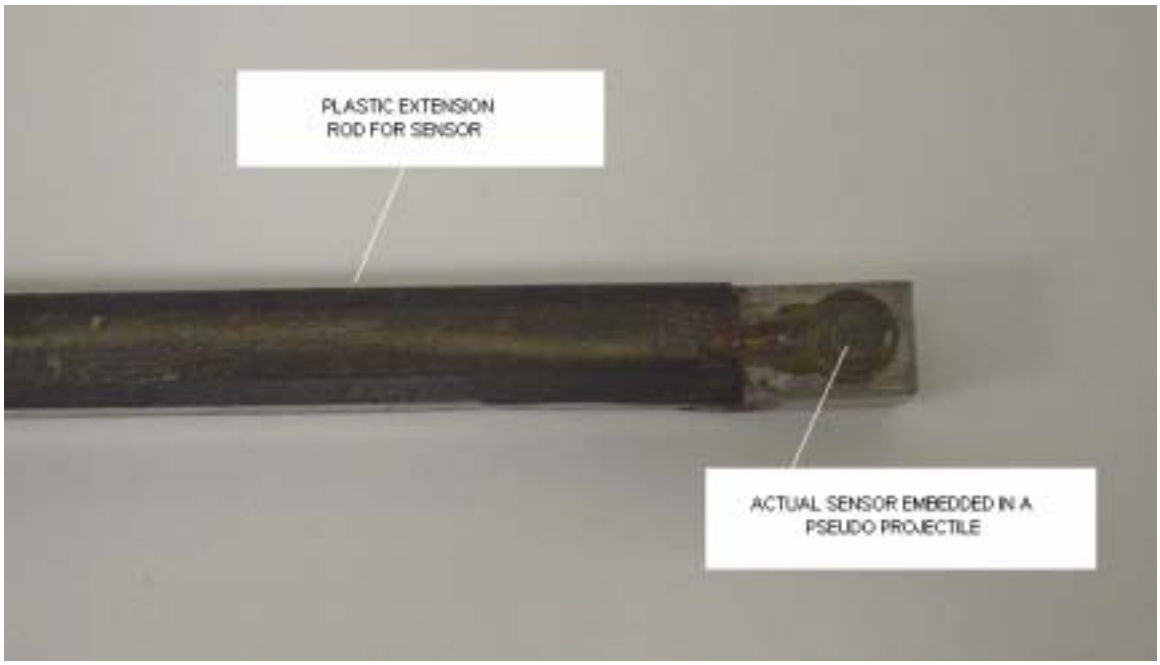

Figure 9. Side view of the Capacitec Non-Contact Capacitive Sensor Embedded into a Pseudo-Projectile.

Figure 10. The Sensor Along with its Plastic Extension Rod.

Figure 11. Capacitec Power Supply.

Capacitec's non-displacement systems use a Series 4000 amplifier with a ± 15V power supply: the sensor produces an analog voltage proportional to the distance between the capacitive probe and rails. The principle of this conversion is based on the capacitive reactance being proportional to the spacing of a parallel plate capacitor. The rails in this capacity, serve as an electrical conductive surface, which are connected to ground to complete a circuit and take measurements. The capacitive reactance is then found by use of an A.C. constant current source and a low capacitance voltage pre-amplifier by measuring the voltage drop across the probe capacitance. The probe voltage is proportional to the probe capacitive

reactance, which is in turn proportional to the probe spacing to the measuring surface. The measured A.C. constant voltage is rectified, synchronously detected, and filtered to give an average D.C. voltage. While the sensing probe is of finite size, it does not appear as a parallel plate capacitor at long distances from the measuring surface, which makes the output become non-linear; therefore, a special linearization circuit is used to extend the sensing probe's linear range. Lastly, the signal is further amplified to give the observed signal [8].

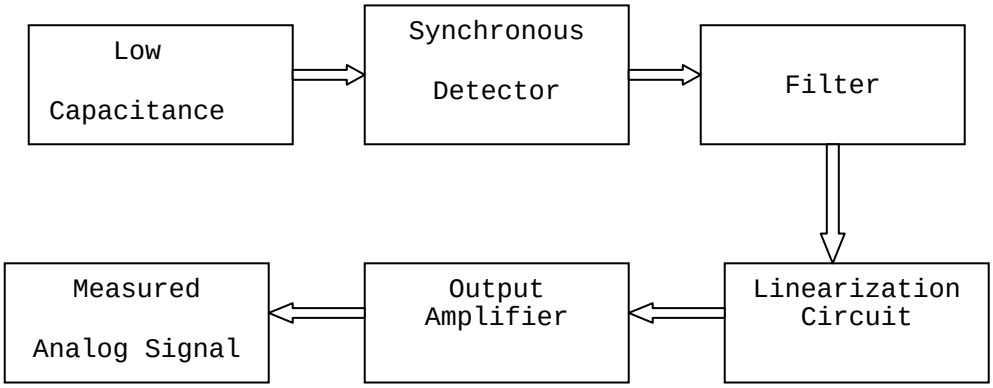

Figure 12. Schematic Block Diagram of the Capacitec Sensor Signal.

The picture below (Figure 13) shows the rails and sensor and also shows the calibration method used daily prior to measuring distance between the actual rails in the assembly. Shown in the picture are two rails with a precision spacer measuring 0.2500 ±0.0001 inches and the inserted sensing probe. This calibration method produces the standard reading for 0.2500 ±0.0001 inches to be used for that particular day. The analog voltage reading given by the Series 4000 amplifier is then converted to a

distance reading by the Bargrafx software in units of microns; 6350 microns is the equivalent of 0.2500 inches.

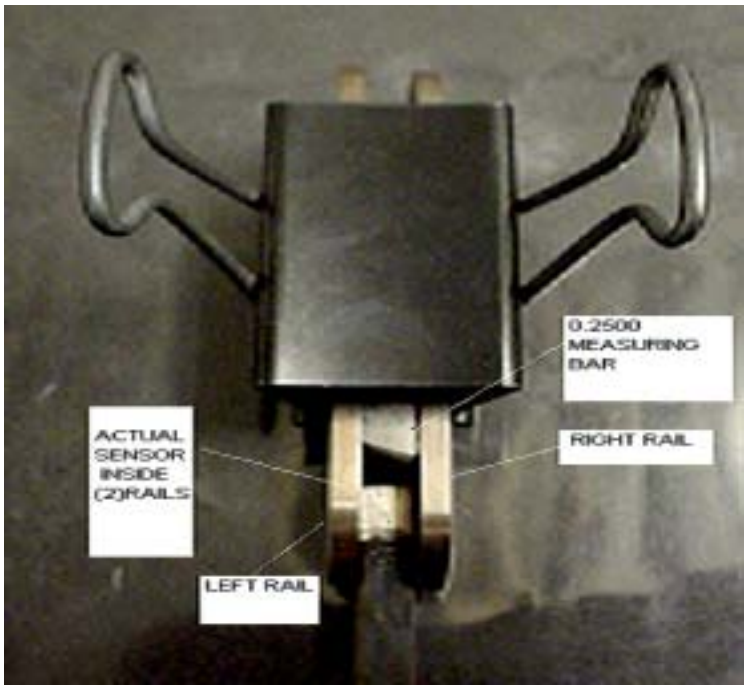

Figure 13. Top View The of the Sensor Placed Inside Two Rails Separated by a 0.2500-in Bar and Held Together by a Paper Clamp (Daily Calibration Method).

From the daily distance measurement acquired, experimental shots were taken with distances between the rail and armature measuring from 7 to 100 μm with equal spacing throughout the length of the rail. Shots were also taken where the measured distance at one end of the 100-cm rails was at a smaller distance (ranging from 5 to 50 μm) than the other.

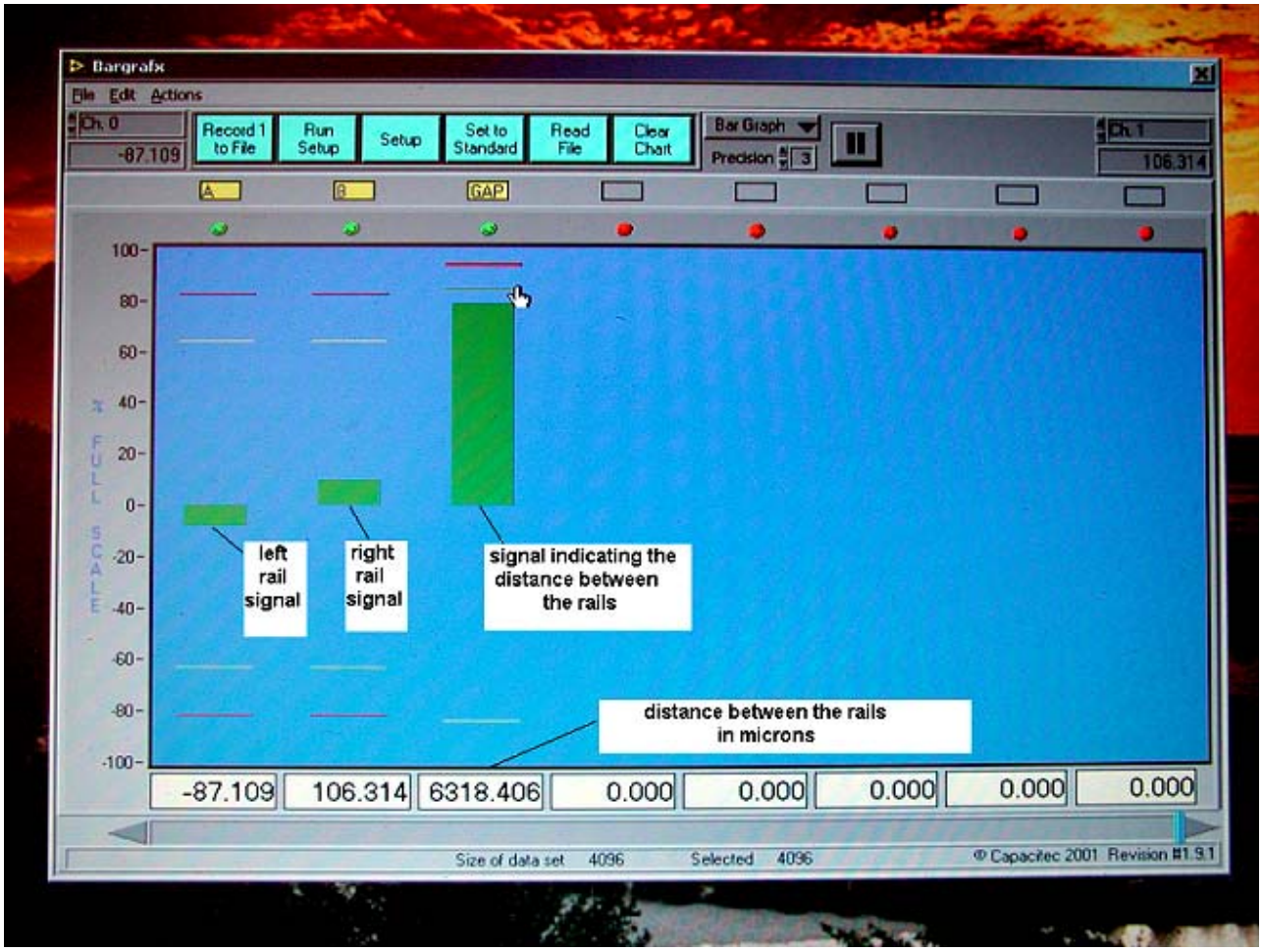

Figure 14. Depiction of Bargrafx Software.

2. Hard Chrome Plating of the Rails

Hardness for the rails used in the NPS rail gun stand can be described by a Rockwell Scale calculation. Rockwell hardness testing is a general method for measuring the bulk hardness of metallic and polymer materials. The material's hardness correlates with its wear resistance, strength, and other properties. The Rockwell hardness test is an indentation test method that takes the comparative depth of two controlled indentations (major and minor loads) in a metal, and superimposes one over the other. The hardness measurement obtained is a representation of how much additional depth the major load has been indented beyond that of the initial indentation of the minor load and is calculated from the depth of permanent deformation [9]. Many scale symbols exist for the Rockwell Scale but for purposes of this thesis, only those listed in Table 1 are of significance. The penetrators in Table 1 are brale (cone-shaped diamond) and hard steel balls with dimension listed below and major and minor loads are defined in units of kgf (1kgf = 1N).

Rockwell Regular and Superficial Scales

ROCKWELL (R) REGULAR SCALE APPLICATIONS			
Scale Symbol	**Penetrator**	**Major (Minor) Load**	**Typical Application**
A	**Brale**	**60 kgf (10 kgf)**	**· cemented carbides · thin steel · shallow case hardened steel**
B	**1/16" Ball**	**100 kgf (10 kgf)**	**· cooper alloys · soft steel · aluminium alloys · malleable iron**
C	**Brale**	**150 kgf (10 kgf)**	**· steel · hard cast iron · perlitic malleable iron · titanium · deep case hardened steel**
D	**Brale**	**100 kgf (10 kgf)**	**· thin steel · medium case hardened steel · perlitic malleable iron**
E	**1/8" Ball**	**100 kgf (10 kgf)**	**· cast iron · aluminium alloys · magnesium alloys · bearing metals**
F	**1/16" Ball**	**60 kgf (10 kgf)**	**· annealed copper alloys · thin soft sheet metal**

Table 1. Rockwell Scale Applications [10].

Copper-tungsten, the metallic alloy used for the rails in previous research, measures 90 – 94 B on a Rockwell Scale hardness scale as noted by Donald Gillich in June 2000 [6]. This particular rail proved to work well along with the use of a commercial silver paste and when sliding electrical contact was maintained throughout the length of the rail. However, breakdown occurred and sliding electrical contact was broken at current densities around 30 kA/cm^2 as observed by Smith in December 2002 [5]. In the

current research, chrome plating was chosen because of its significantly greater hardness on the Rockwell scale. Chrome plating on the Rockwell C scale is listed as around 68 – 75 C. The two hardness measurements cannot be compared due to the B and C scale symbol difference, but the difference is a numerical value of approximately 70. For example, 115 on a B scale is the equivalent of 45 on the C scale [10]. From this simple interpretation, we see that chrome plating greatly surpasses the hardness of copper-tungsten. Two different chrome-plating approaches were observed in this thesis. The first was the chrome–plating of the previously tested copper-tungsten alloy shown below.

Figure 15. Chrome-plated Copper-Tungsten Rails (Plating done by Barken’s Hard Chrome in Compton, California).

The second approach was to apply the chrome plating technique to an all copper rail (shown below in Figure 16) and take experimental shots testing its durability. The set of rails shown below differ from those shown in Figure 15 by its thinner groove pattern. However, the rails shown below were used for the majority of the shots taken in this thesis (~90) at currents ranging from 13 – 21 kiloamperes.

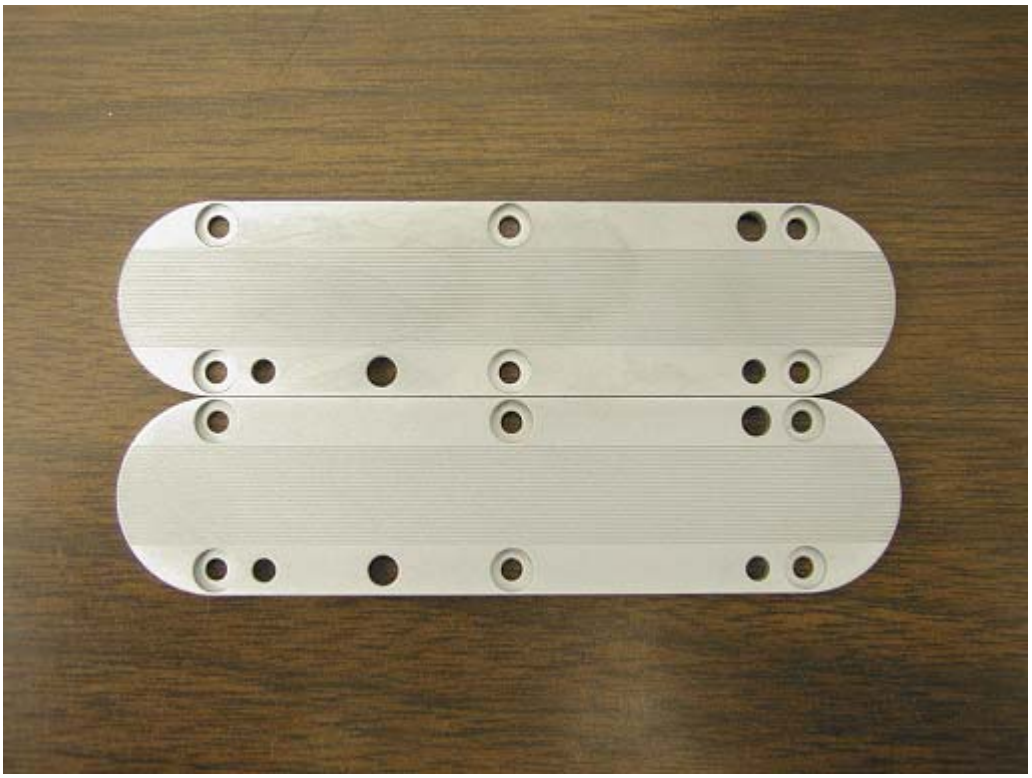

Figure 16. Barken's Hard Chrome-Plated Copper Rails.

THIS PAGE INTENTIONALLY LEFT BLANK

III. TEST RESULTS

A. TEST RESULTS FROM THE ADDITION OF THE SENSOR

Smith's observations and conclusions in December 2002, suggested that non-uniform rail spacing contributed to transition phenomena for experimental shots taken with the NPS rail gun test stand [5]. Capacitec's non-contact capacitive sensor was purchased in order to achieve uniform rail spacing for the NPS rail gun stand, which would hopefully allow for the maintenance of low voltage contact for the projectile's path through the 100-cm long rails. However, test shots taken during this thesis suggests that although rail spacing may contribute to the phenomena of low voltage contact, it is not the sole factor influencing the lack thereof for the NPS rail gun test stand.

The following is a table representing the results from nearly 100 shots. Low-voltage electrical contact failed 90 percent of the time. We see from this table that even at the minimum current density tested, rail damage occurred when contact was broken. It is imperative that low voltage electrical contact be maintained. The semi-liquid conductive coating does not provide adequate protection if low-voltage contact is not maintained. It can also be noted from the table below that there is a shift in rail damage from the front/negative rail, to the back/positive rail at current densities above ~ 25 kA/cm^2.

Damage sustained Front Rail (-)	Damage sustained Back Rail (+)	Current Density $J = \left[\frac{kA}{cm^2}\right]$
Significant	Minimal	25
Minimal	Significant	28
Minimal	Significant	30
Minimal	Significant	32
Minimal	Significant	35

Table 2. Represents Rail Damage Sustained When Low Voltage Electrical Contact is Broken; Data Extracted from Nearly 100 Experimental Shots.

Shots were taken using various methods of setting rail spacing to determine which would promote maintaining optimal electrical contact. As previously stated, gap distances ranging from 7 – 100 μm greater than the width of the projectile were used to set spacings between each type of rail; unfortunately, no trend in improving electrical contact was obtained. It was observed, however that electrical contact was maintained during the beginning of the projectile's travel and was maintained throughout nearly 60 percent of the rail, but near the end, low voltage electrical contact was broken.

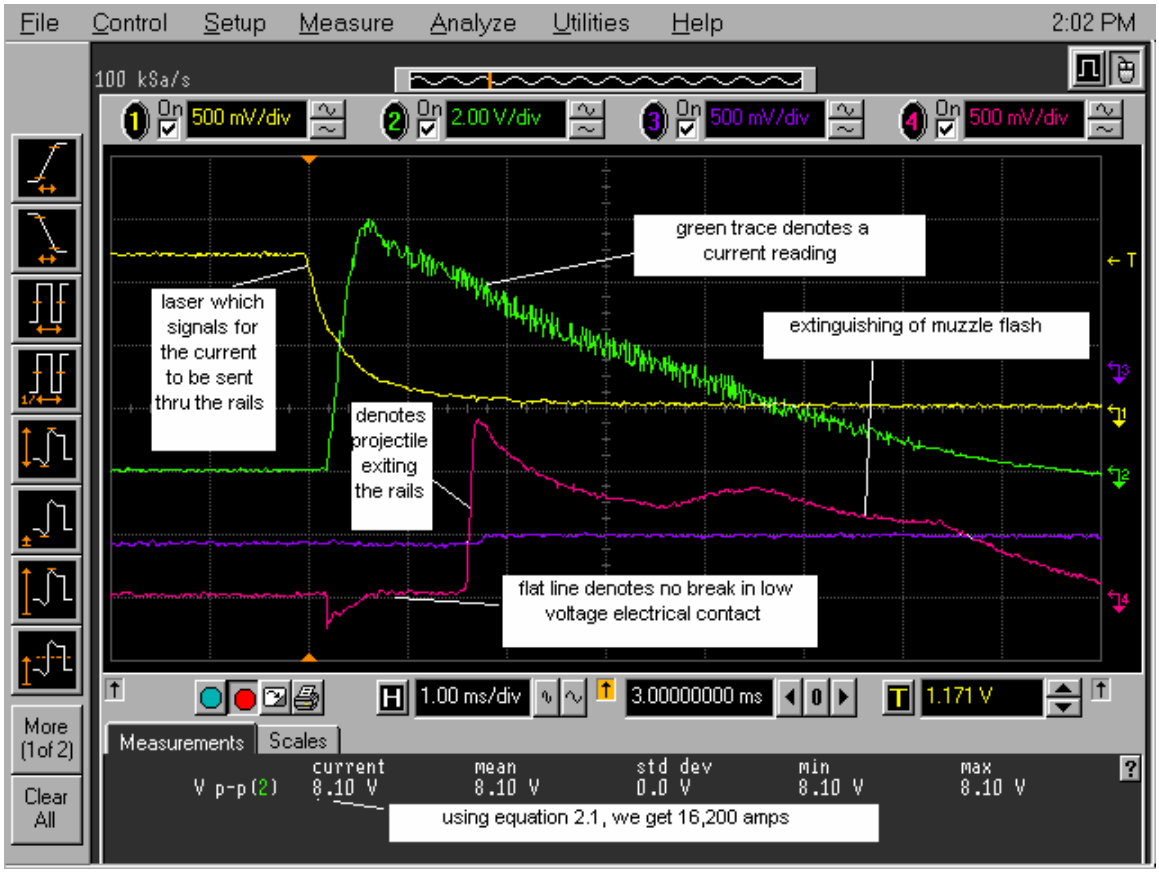

Figure 17. Oscilloscope Reading Illustrating Good Low Electrical Contact using a Gap Distance Beyond the Width of the Projectile of Approximately 50 μm.

Figure 17 above depicts a readout for an ideal shot in the NPS rail gun test stand observations. We see, in the above figure, that the differential amplifier reading (pink waveform) is flat, which denotes no break in sliding electrical contact, until the projectile exits the rails. The yellow waveform shown above represents the laser actually triggering for current to be sent through the rails when the pusher assembly interrupts the light path between the fiber optic cables shown in Figure 6; the green waveform corresponds to the amount of current sent through the rails and measured by the Pearson transformer; and

lastly the purple waveform represents the time at which crossing of the photo-detector and laser beam (seen in Figure 8) by the projectile occurred (Figure 17 indicates a null reading by the purple waveform). The method used to obtain this readout is reproducible; however, the results prove not to be consistent, contrary to what was hoped for in setting highly controlled rail spacings.

Figure 18 below is a depiction of an oscilloscope reading where a break in low-voltage contact is seen. We see the pink waveform in this instance is not uniformly flat after its slight dip as compared to that seen in Figure 17, which denotes the break in contact. This break in contact is an indication to us that damage has occurred to the rails and is observed in Figure 19. The damage sustained to the rail is a result of the amount of power dissipated *P,* which is determined by the following:

$$P = IV \tag{3.1}$$

where *I* is the current calculated from equation 2.1 and *V* is the voltage drop across the rails. In the case of Figure 18, the current ~ 17.5 kA and the voltage drop across the rails is determined to be 25 volts, (the pink waveform below rises to ~ 125 mV and is multiplied times 200, which is a factor derived from an attenuation signal given by the previously discussed differential amplifier), thus making the total power dissipated ~438 kilowatts from equation 3.1. This significant amount of power is what causes damage to rails depicted in Figure 19.

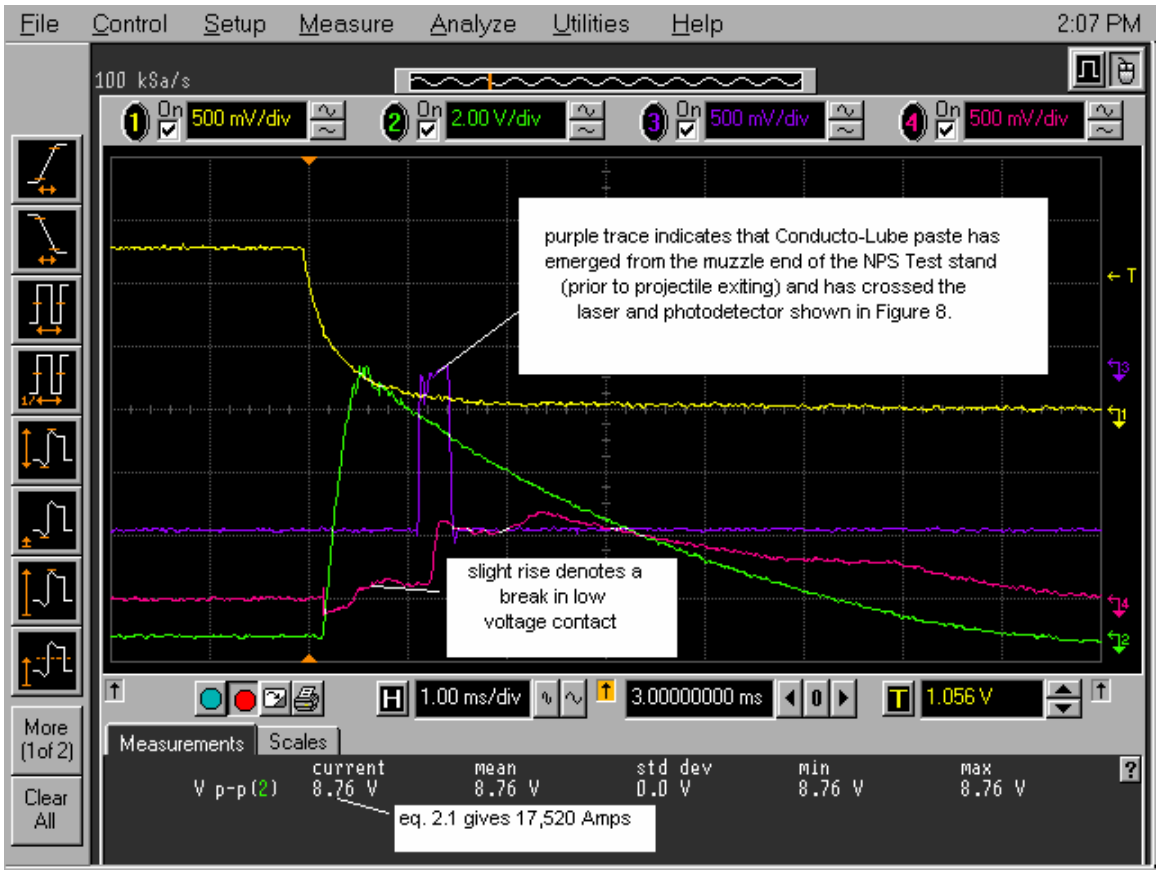

Figure 18. Illustration of Rise in Differential Amplifier Waveform which Indicates a Break in Low Voltage Electrical Contact.

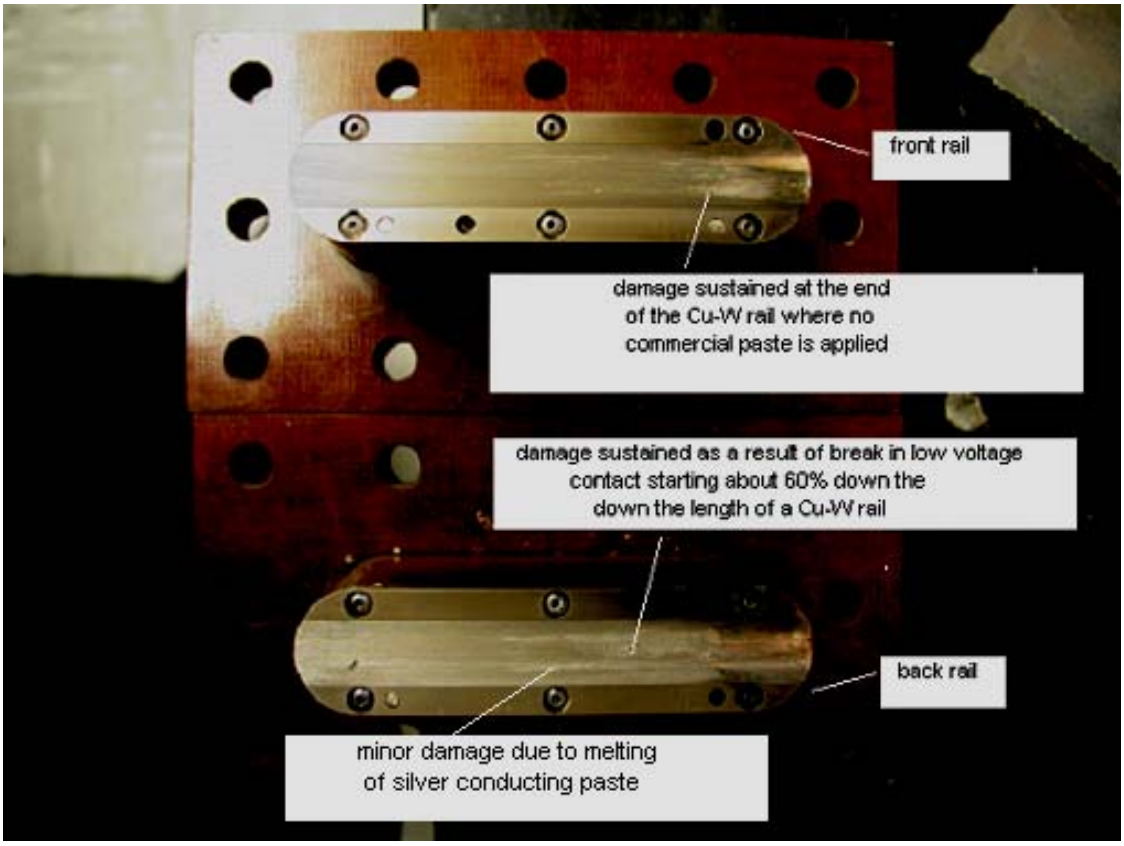

Figure 19. Depiction of Corresponding Rail Damage Sustained from the Oscilloscope Reading in Figure 18.

We thought that if the rail spacing was set reasonably tight, low-voltage electrical contact would possibly be maintained due to the slight physical contact between the rail and projectile. The results from this approach are shown in Figures 20 and 21.

Figure 20. Illustration of Tight Rail Spacing between the Projectile and Rails.

Figure 20 depicts data obtained for a shot with a gap distance between the projectile and rails of about 5 μm, while Figure 21 below depicts is corresponding rail damage. There is only a slight rise in the differential amplifier waveform readout but its length tells us that the projectile was slowed down during its travel while inside the rails. The computed velocity of the projectile in this instance was 21.7 m/s while the average velocity for most shots taken was approximately 50 m/s. In this case, the gap distance between the rail and projectile was so small that the projectile's velocity slowed significantly.

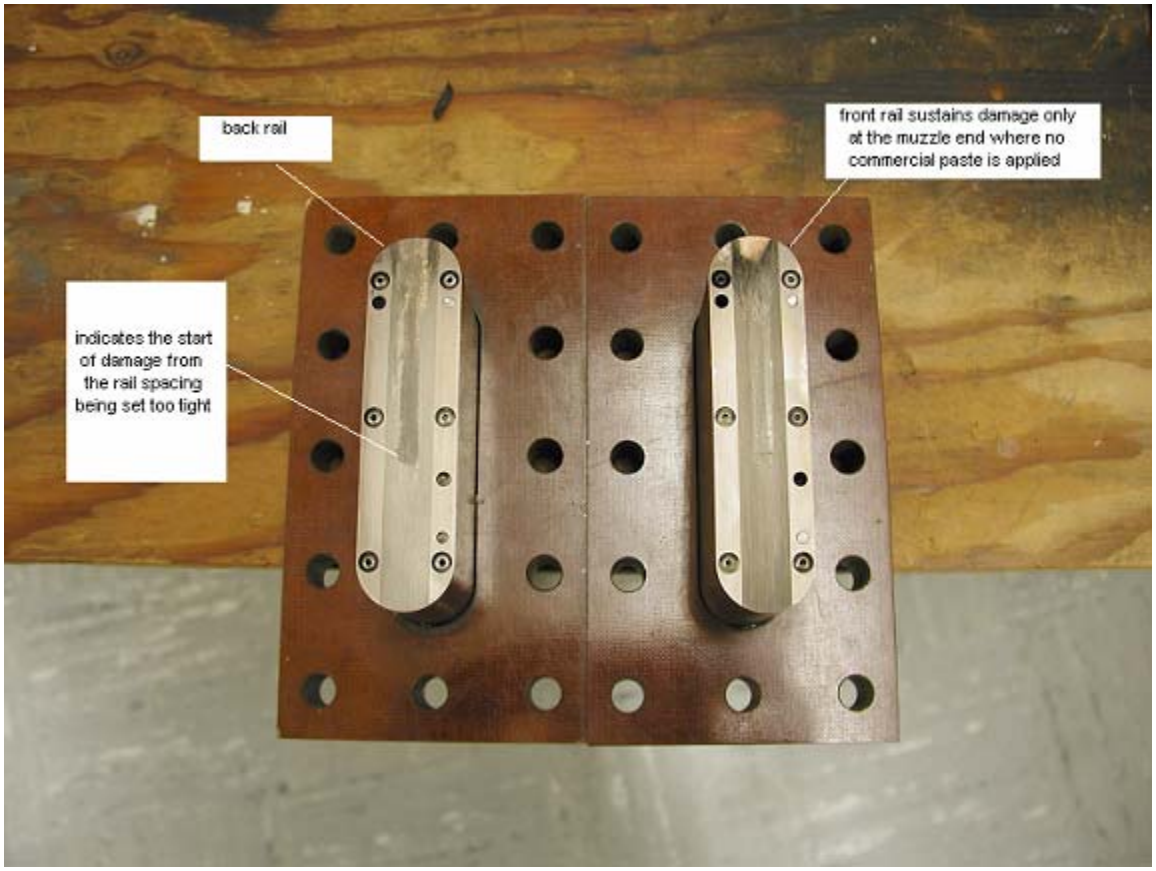

Figure 21. Depiction of Rail Damage Corresponding to Oscilloscope Reading in Figure 20 (Gap Distance between Rails and Projectile is set to ~ 5 μm).

THIS PAGE INTENTIONALLY LEFT BLANK

B. TESTS RESULTS FROM HARD CHROME PLATING THE RAILS

Hard chrome plating was used to try to reduce rail damage. Two different chrome-plating approaches were considered. The first was a chrome-plated copper-tungsten rail and the second was a chrome-plated copper rail. However, it was observed from conducting experimental shots with both chrome-plated copper and copper-tungsten, that regardless of metallic rail make-up, damage will indeed occur if low voltage electrical contact is not maintained.

The chrome-plated copper rail did not hold up well at all due to copper's low melting point (1083 degrees Celsius). The damage seen in Figure 22 indicates that arcing occurred and produced temperatures that exceeded the melting point of copper. A similar inference can be made from the corresponding oscilloscope traces depicted in Figure 23. The damage seen in Figure 22 corresponds to a shot with a current density of 28 kA/cm^2. As usual, damage occurs on the back/positive rail and little or no damage is observed on the front/negative rail. Also, consistent with the shots is approximate location of where the damage begins; this is consistently just past the half-way mark of the length of the rail.

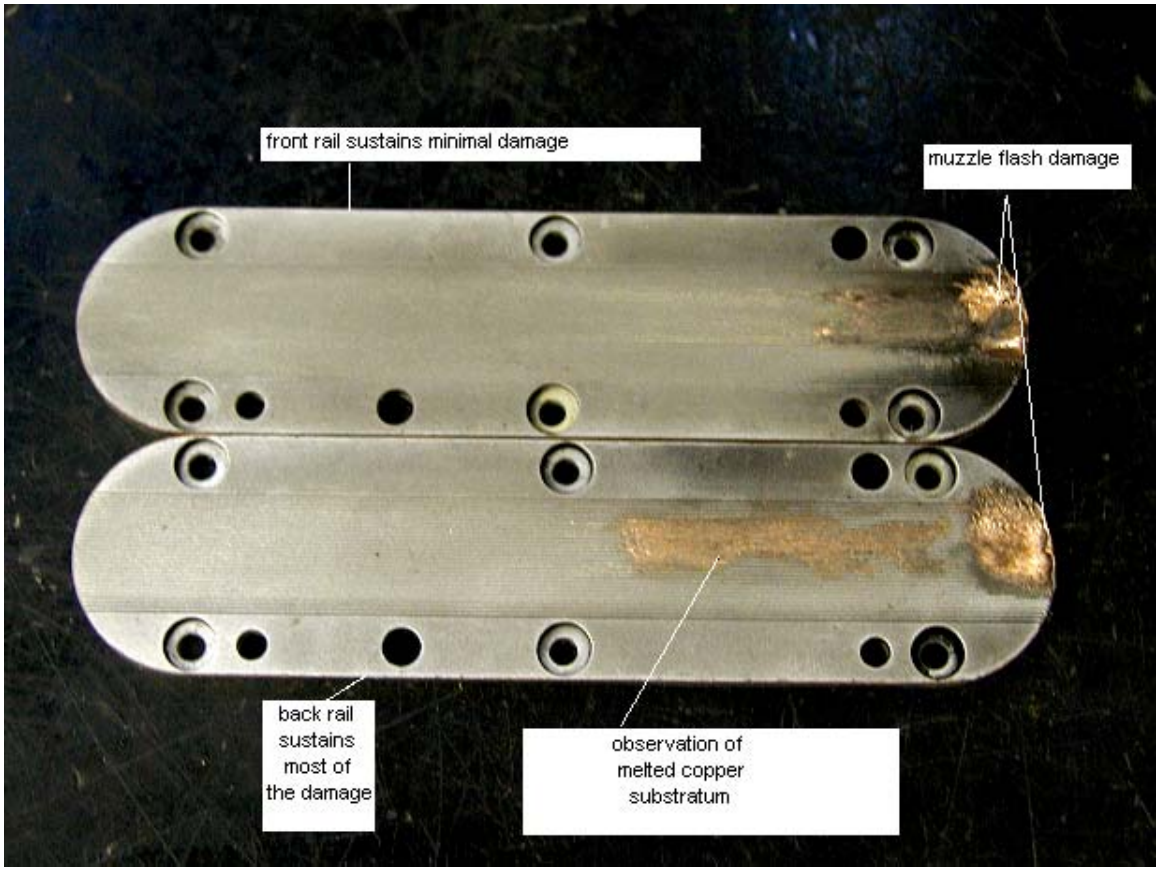

Figure 22. Damage Sustained to Chrome-plated Copper Rails (Plating Done by Barken's Hard Chrome in Compton, California).

Figure 23. Depiction of Oscilloscope Reading Corresponding to Rail Damage in Figure 22.

Damage was also sustained to the chrome-plated copper tungsten rail, however its damage was not as severe. The Cu-W chrome plated rail damage seemed to be only a few chipped chrome plated portions, but no significant damage to the rail itself, only the plating. The oscilloscope traces and photographs of the corresponding rails are shown in Figures 24 and 25.

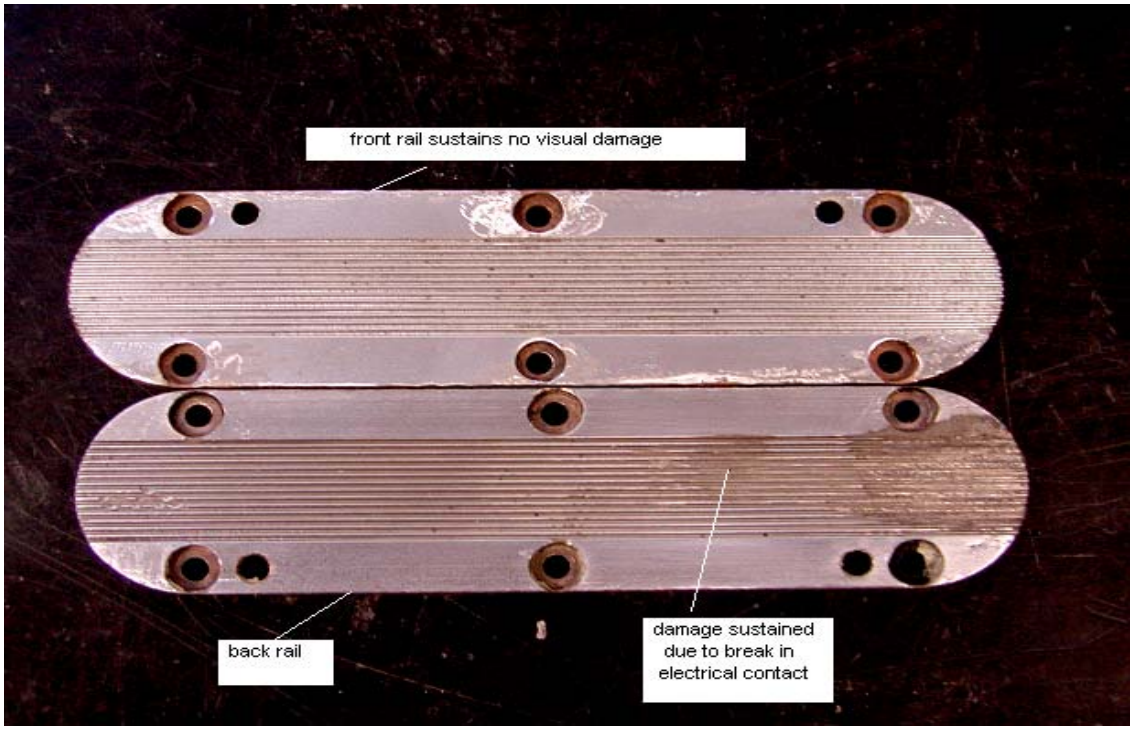

Figure 24. Copper-Tungsten Chrome-Plated Rail.

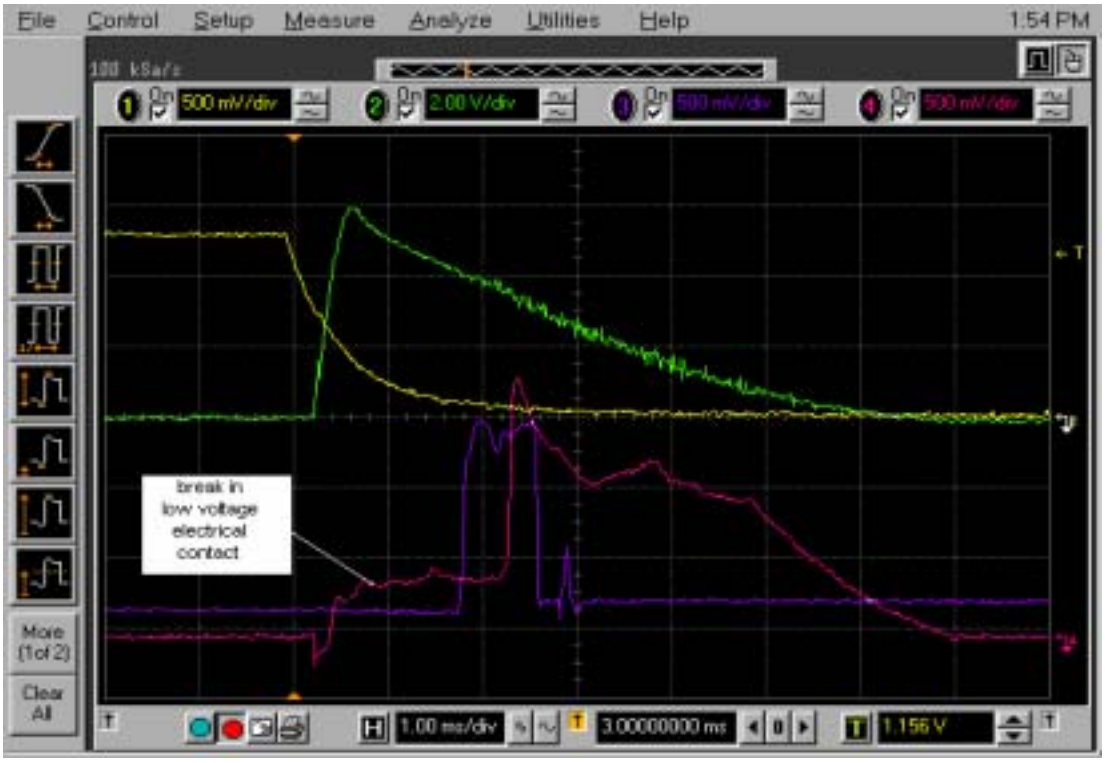

Figure 25. Depiction of Oscilloscope Reading Corresponding to Rail Damage in Figure 24.

C. SUMMARY OF RAIL DAMAGE ANALYSES FROM TEST RESULTS

During this thesis work, the NPS rail gun test stand was fired nearly 100 times; sometimes without the silver-based conducting paste (Conducto-Lube), but most times with it. Without the conductive paste as an interface, considerable damage is sustained on both rails even at low current densities (20 - 22 kA/cm^2), as shown in Figure 26.

Figure 26. Damage Sustained with No Silver Paste Interface (Conducto-Lube)

When the conducting paste was used as a rail-projectile interface, damage was significantly reduced, as shown below in Figure 27.

Figure 27. Photograph Taken After a Shot When Paste Was Applied and Low-Voltage Contact Maintained.

It can be also be concluded from these experiments that when low-voltage contact is broken, extensive damage occurs on the front/negative rail for current densities of $\leq$ 25 kA/cm^2 and shifts to the back/positive rail for current densities > 25 kA/cm^2, as shown in Table 2. Results also show that breaks in low voltage electrical contact occur usually just past the halfway point along the length of the rail (shown is Figures 19, 22, and 24) for all shots except where the gap distance between the rail and projectile was too tight (Figure 21 shows damage beginning just prior to the halfway mark).

THIS PAGE INTENTIONALLY LEFT BLANK

IV. CONCLUSIONS

The addition of Capacitec's non-contact capacitive sensor and its effect of obtaining parallelity and uniform rail spacing for the NPS rail gun test stand may somewhat contribute to the maintenance of low-voltage electrical contact, but definitely is not the sole factor contributing to the lack thereof. The hard-chrome plating of the copper-tungsten rail sustains minimal rail damage even when low voltage contact was broken. The phenomena of low voltage electrical contact and the actual transitioning processes occurring inside the rails should be more closely examined to further understand what will reduce the breakdown in contact being observed. Once full knowledge of processes occurring inside the rail is understood, and low-voltage electrical contact is maintained, the chrome-plated copper-tungsten rail should be further tested at current densities ranging from 30 – 50 kA/cm^2 and at projectile velocities greater than the 70 m/s used in this thesis.

THIS PAGE INTENTIONALLY LEFT BLANK

LIST OF REFERENCES

1. Petry, C.R., *Hypersonic Naval Railgun,* Naval Surface Warfare Center, Dahlgren, Virginia, April 2003.

2. Fair, H.D., Gora, T.F., Kemmey, P.J., *Proposal for the Development of Electromagnetic Guns and Launchers,* Propulsion Technology Laboratory Technical Department, Applied Sciences Division, Arradcom, Dover, New Jersey, 1978.

3. Stefani, F., Levinson, S., Satapathy, S. Parker, J., *Electrodynamic Transition In Solid Armature Railguns,* Ieee Transactions On Magnetics, Vol. 37, No. 1, 2001.

4. Culpeper, W.C., *Rail Erosion and Projectile Diagnostics for an Electromagnetic Gun,* Master's Thesis, Naval Postgraduate School, Monterey, California, June 2002.

5. Smith, M.W., *Barrel Wear Reduction in Rail Guns: An Investigaion of Silver Paste Liquid-Metal Interface,* Master's Thesis, Naval Postgraduate School, Monterey, California, December 2002.

6. Gillich, D.J., *Design, Construction, and Operation of an Electromagnetic Railgun Test Bench,* Master's Thesis, Naval Postgraduate School, Monterey, California, June 2000.

7. Adamy, M.T., An Investigation Of Sliding Electrical Contact in Rail Guns and the Development of Grooved-Rail Liquid-Metal Interfaces, Master's Thesis, Naval Postgraduate School, Monterey, California, December 2001.

8. Capacitec, Operation/Maintenance Manual for Series 4000 Capacitec Amplifiers and Rack Accessories, Capacitec, Incorporated, Ayer, Massachusetts, January 1998.

9. **WWW.MEE-INC.COM/ROCKHAR.HTML**, *Rockwell Hardness Testing,* Materials Evaluation and Engineering, Incorporated, Plymouth, Minnesota, April 2003.

10. **WWW.CCSI-INC.COM**, *Technotes: Basics Of Rockwell Hardness Testing,* Corporate Consulting, Service & Instruments, Incorporated, Akron, Ohio, April 2003.

APPENDIX A

RAIL DRAWING (1)-WIDE GROOVES

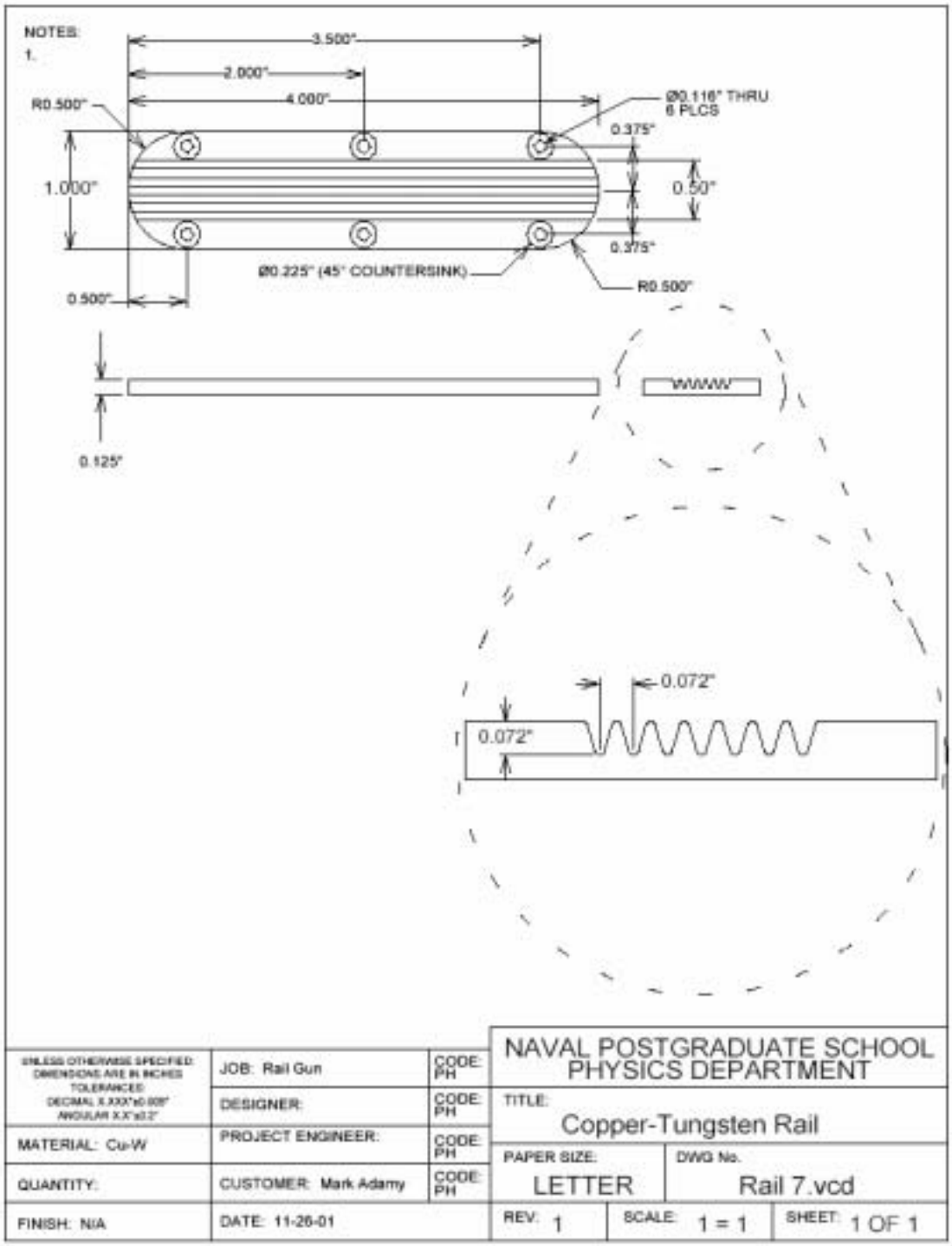

RAIL DRAWING (2) – THINNER GROOVES

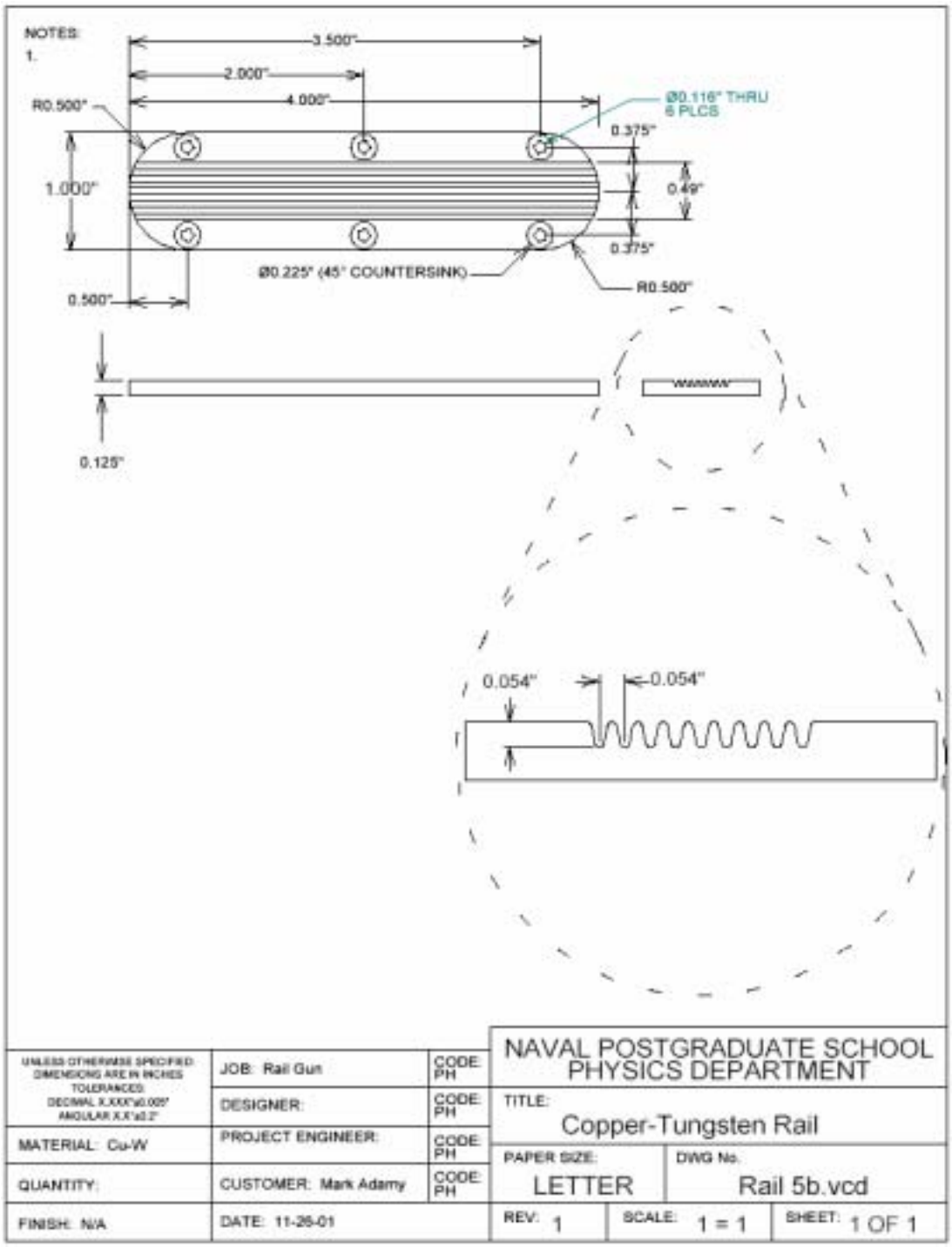

INITIAL DISTRIBUTION LIST

1. Defense Technical Information Center
   Ft. Belvoir, Virginia

2. Dudley Knox Library
   Naval Postgraduate School
   Monterey, California

3. Professor William B. Maier II, Code PH/Mw
   Department of Physics
   Naval Postgraduate School
   Monterey, California

4. Professor Richard Harkins, Code PH
   Department of Physics
   Naval Postgraduate School
   Monterey, California
5. Lab Director Don Snyder, Code PH
   Department of Physics
   Naval Postgraduate School
   Monterey, California

6. Engineering Curriculum Officer, Code 34
   Department of Physics
   Naval Postgraduate School
   Monterey, California

7. Commander Roger D. McGinnis
   NAVSEA Washington, D.C.
   PMS 405, Program Manager
   Washington, D.C.

8. Fred Beach
   NAVSEA Washington, D.C.
   PMS 405/Code N13
   Washington, D.C.